ECCOMAS Congress 2016
VII European Congress on Computational Methods in Applied Sciences and Engineering
M. Papadrakakis, V. Papadopoulos, G. Stefanou, V. Plevris (eds.)
Crete Island, Greece, 5–10 June 2016

SIMULATING ATOMIC FORCE MICROSCOPY FOR THE DETERMINATION OF THE ELASTIC PROPERTIES OF NANOPARTICLE REINFORCED EPOXY RESIN

Johannes Fankhänel*[1], Andreas Kempe[1], and Raimund Rolfes[1]

[1] Institute of Structural Analysis, Leibniz Universität Hannover
Appelstraße 9a, 30167 Hannover, Germany
*e-mail: j.fankhaenel@isd.uni-hannover.de

Keywords: Molecular Dynamic Finite Element Method (MDFEM), Computational Mechanics, Nanocomposite Simulation, Elastic Properties, Atomic Force Microscopy (AFM)

Abstract. *Nanoparticles show a great potential in improving especially the matrix-dominated mechanical properties of fiber reinforced plastics, like compressive strength or impact tolerance. The composition of the interphase between nanoparticles and the surrounding matrix is assumed to be of vital importance for the mechanical properties of the composite material. Characterizing nanoparticle-matrix interphases with experimental methods, e.g. using atomic force microscopy (AFM), is highly complex and time consuming. Therefore an AFM-simulation technique based on the Molecular Dynamic Finite Element Method (MDFEM) is introduced. The MDFEM provides a powerful method for simulating molecular dynamic problems within the finite element framework, perspectively allowing for the efficient simulation of multi-scale models and pure FE-models in order to reduce the numerical cost for bigger problems. With the presented method, the elastic properties of pure boehmite particles as well as pure epoxy resin have been determined and are in good agreement with experimentally obtained values. The influence of different particle-matrix interactions on the elastic properties of the interphase has been studied for unmodified boehmite particles. Supporting virtual tensile tests on cubic unit cells show outstanding accordance with experimental results. The presented method can contribute to the optimization of nanocomposite materials and at the same time reduce the need for experimental effort.*

1 INTRODUCTION

Carbon fiber composites are regarded as one of the most important lightweight construction materials for the future. By incorporating nanoparticles, it is possible to improve the properties of the weak constituent of the composite material, i.e. the matrix material. Arlt [1] shows that unmodified and taurine modified boehmite particles are able to improve matrix-dominated properties of carbon fiber/epoxy composites, like shear strength, shear modulus, compressive strength or compression after impact strength by 10 to 25 %. Other studies show similar results. Uddin & Sun [2] investigate silica particles in a glass/epoxy composite and report significant improvements regarding the compressive strength and modulus as well as the tensile strength perpendicular to the fiber direction. Subramaniyan & Sun [3] obtain similar results for a nanoclay/glass/epoxy composite.

In contrast, there are studies that report negative effects, especially for higher particle weight fractions. Shahid et al. [4] investigate boehmite particles with two surface modifications (lysine and para-hydroxybenzoate) in a carbon fiber/epoxy composite and report an increase of tensile and flexural properties for very small particle fractions. For weight fractions above approximately 5 %, the properties decrease compared to the unfilled composite. Siddiqui et al. [5] observe partly increased properties for nanoclay composites, like flexural modulus and fracture toughness and partly decreased properties, like flexural strength and impact toughness.

Comparing the results of these investigations, it can be concluded that the composition of the interphase between nanoparticles and matrix is of vital importance for the mechanical properties of the composite. This becomes especially obvious, when considering that Arlt and Shahid et al. investigate a similar boehmite/epoxy material combination, but with different particle surface modifications and achieved completely different results. Following the argumentation of Arlt, nanoparticles and their surface modifications highly influence the morphology of the surrounding matrix by impeding the cross-linking reaction and thus forming a soft interphase around the particles. Thereby two mechanisms may occur. Firstly, hydroxyl groups on the particle surface are assumed to be able to react with epoxy groups of the matrix during the curing reaction instead of hydroxyl groups of the matrix. This should lead to approximately the same amount of cross-links as compared to the undisturbed matrix. However, some of those cross-links are formed between particle and matrix instead of between prepolymer chains, resulting in an improved particle matrix interaction and in a softer matrix material. As a second possibility, the hydroxyl groups on the particle surface are assumed to be able to react with the prepolymer chains through etherification even before the hardener is added to the uncured matrix. Thus, many epoxy groups in the matrix near the particle surfaces are already occupied and no longer available for further reactions during the curing reaction, leading to a lower cross-linking density between prepolymer chains in this area. This should again lead to an improved particle matrix interaction at the cost of a soft matrix material around the particles. These phenomena have been substantiated in the work of Arlt by Atomic Force Microscopy experiments. It has been found that unmodified boehmite particles exhibit the aforementioned surrounding ring of soft material in the ambient matrix.

AFM is often used to validate molecular dynamics simulations but rather less literature on molecular dynamics AFM simulations of the indentation behavior is available. Many studies focus on characterizing the adhesion and separation behavior. Landman et al. [6] for example simulate adhesion and separation during the indentation of a nickel tip in a gold sample. Other studies, like Fang et al. [7], apply molecular dynamics AFM simulations to the investigation of the lithography process, in this case of crystalline copper with good agreement with experimental results. Still other studies investigate pull out processes, e.g. Heymann and

Grubmüller [8] perform single molecule atomic force microscopy simulations by pulling out a hapten molecule of a ANO2 binding pocket. In the present study, atomic force microscopy simulations in order to investigate the elastic properties of particle-matrix interphases are presented. The specific goal is to gain evidence for the discussed mechanisms and to validate the assumptions in the generation process of the models in a scale specific manner.

This paper is structured as follows: Starting with a short summary of the chosen simulation method (MDFEM), the generation process and the AFM simulation model is introduced in section 3. The numerical investigations presented in section 4 comprise two steps. The first step of the work presented includes AFM simulations, in which particle and matrix are analyzed separately. These preliminary investigations are used for the calibration and optimization of the AFM models. Different parameters like tip and sample size or boundary effects are analyzed. The second part deals with the actual characterization of the particle-matrix interphase. AFM simulations on samples consisting of both particles and matrix material as well as particle-matrix interphases are performed for a composite material comprising an anhydride-cured epoxy matrix and unmodified boehmite particles. The effect of three different particle-matrix interactions on the mechanical properties of the interphase is investigated and evaluated on the basis of intensive parametric studies. The results are discussed in the context of simulated tensile tests of the material combinations mentioned earlier.

2 THE MOLECULAR DYNAMIC FINITE ELEMENT METHOD

In this chapter, a brief overview of the Molecular Dynamic Finite Element Method (MDFEM) is given. For a more detailed presentation, the reader is referred to earlier work of the senior authors of the present paper [9, 10].

The MDFEM can be regarded as a framework to perform classical molecular dynamics (MD) simulations by means of the well-established finite element method (FEM). The main motivation for this approach is the simplification of multi-scale techniques, as for example the coupling of atomistic and continuum mechanics simulations can be performed in a very efficient way within one software package. Additionally, the need for special in-house developed software is reduced, since FEM software mostly comes with highly efficient solvers and pre- and post-processing tools.

When thinking of molecular structures as multi-body systems, where atoms are point masses and bonds are springs, the FEM seems to provide an appropriate framework for MD simulations, since structural elements such as trusses, beams and springs are an integral part of FE codes. A variety of such MD-FE models has been proposed for the simulation of graphene, see for example Wang [11], Zhang et al. [12] and Zhu et al. [13]. Nevertheless, there are some challenges or problems when applying standard truss or beam elements to general MD problems. The use of truss elements seems to be reasonable at the first glance, since nodes of truss elements similarly to atoms only have translational degrees of freedom. However, usual MD bending potentials require the introduction of either rotational springs and truss angles between two truss elements or normal springs between two connected outer nodes of the angle. Normal springs in turn, can only reproduce the bending potentials through very complex geometric relations for large deformations. Additionally, truss elements cannot reproduce torsion or inversion MD potentials, which makes truss elements only applicable for planar structures or special spatial structures, where torsion and inversion do not occur. Due to the lack of torsional stiffness, those models are also relatively instable.

An alternative approach is the approximation of bonds by means of standard beam elements. Many different models have been made proposed, like using e.g. rigidly connected beams or joints and constrained rotational degrees of freedom. Examples can be found in Li [14], Chwal et al. [15] and Flores et al. [16]. The main problem when using these models is

the determination of the beam constants. While normal stiffnesses can be calculated directly from the bond stretch potentials, bending stiffnesses can only be derived unambiguously for special cases, like planar structures, where torsion can be neglected. The reason for this behavior stems from the fact that torsion between two planes can also be expressed through bending of elements. Even for planar structures the beam element method can lead to wrong results, since beam rotations are transferred from beam to beam through the structure.

Even though it is possible to obtain the correct behavior with a certain superposition of rigidly and flexibly connected beam elements, as shown in [10], the MDFEM provides a more elegant method, using special 2-, 3- and 4-node elements for bond stretch and physical interactions, bending and torsion. By superposing those elements, various atomistic problems can be modeled. Advantages of the MDFEM, compared to the aforementioned approaches include automatic model relaxation due to intrinsic equilibrium parameters, the possibility of easily calculating large deformations and reproducing multiple equilibrium positions as well as a reduced numerical effort due to the elimination of the rotational degrees of freedom. Disadvantageous is the comparatively high effort to generate simulation models. Sample applications of the MDFEM include carbon nanotubes [9] as well as elastomers [17].

3 MATERIALS AND MODELS

The studies presented in the following chapters focus on boehmite nanoparticle-reinforced epoxy composites. The chemical structure of boehmite (γ–AlO(OH)) is assumed to be of the cmcm unit cell (see Figure 1 a)), as reported by Bokhimi et al. [18] and experimentally confirmed through X-ray diffraction carried out at the Institute for Particle Technology of the TU Braunschweig [19]. The primary particle size of the particles is in the range of 14 Å and the particles have an orthorhombic shape, as shown in Figure 1 b). The AFM tip material is silicon with an Fd3m (diamond) unit cell.

The matrix material is an epoxy resin based on Bisphenol-A-diglycidylether (DGEBPA) prepolymer chains and a Methyl-Tetrahydrophthalic Anhydride (MTHPA) hardener. Both chemical structures are shown in Figure 1 c) and d) respectively.

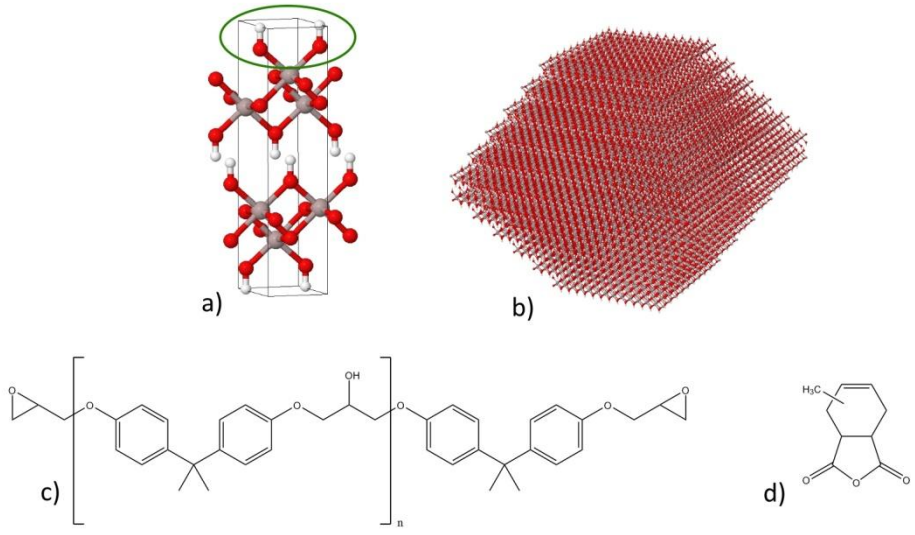

Figure 1: a) Crystallographic unit cell of cmcm boehmite; b) Orthorhombic shape of the boehmite particles; c) Chemical structure of DGEBPA prepolymer chains; d) Chemical structure of MTHPA hardener.

All models are generated with in-house software using Open Babel [20] and Packmol [21]. In a first step, the particle is created by duplicating the boehmite unit cell and cutting out the shape of the particle. Afterwards, prepolymer chains are randomly packed into the simulation box around the particle. Subsequently, the ester cross-links are created. The algorithm randomly iterates over all hydroxyl groups. If an epoxy group within a specified search radius is found, a hardener molecule is placed and connected. If multiple epoxy groups are found, the algorithm always uses the closest one. If all hardener molecules are placed or no more reaction partners are found, the same process is executed for the etherification reaction. Finally, the AFM-tip is created and placed, again by duplicating the silicon unit cell and cutting out the hemispherical shape.

Concerning the particle-matrix-interphase, three different variations are compared. All three variations are based on an unmodified boehmite particle. As a first variation, the particle is assumed to interact with the matrix only by physical interactions. In the second variation, the particle is bonded both physically and chemically. The surface hydroxyl groups of the boehmite (highlighted in Figure 1 a)) are enabled to develop covalent bonds to the epoxy groups of the matrix material by joining the cross-linking reaction. The third variation follows the argumentation of Arlt [1], that interphases around the particles can develop even before the epoxy is cured. To take this into account, a preliminary etherification step only for particle hydroxyl groups is inserted. Afterwards, the ester and ether connections for the remaining reactive sites are created. The three variations in the mentioned order are denoted as variation 1, 2 and 3 in the following.

All simulations presented in this study are performed using the MDFEM in combination with the Dreiding force field [22]. Even though it is possible to apply different cutoff radii for the physical interactions within the sample and between sample and tip, a cutoff of 15 Å has proven to be suitable for both cases by parametric studies. The tip itself is considered to be rigid, meaning that all chemical and physical interactions within the tip are eliminated, by removing the corresponding elements. Since real AFM tips are deformable, this has to be considered in the calculation of the elastic modulus of the sample (see chapter 4). The first step in the simulations is, as usual in molecular dynamics calculations, the determination of the equilibrium state of the system. Therefore, the whole model including the AFM tip is relaxed over a varying period of time ranging from 50 to 200 ps, depending on the model size. In the relaxation step, the equilibrium position of the tip (in the sense of the tip lying on the sample surface without cantilever forces) is obtained automatically. Subsequently, the load is applied in terms of a displacement of the tip by 0.5 to 1.5 nm, depending on the sample and tip size. A simulation time of 300 ps has proven to be suitable by parametric studies. All samples are constrained on all surfaces in a border region of 0.2 nm, except for the top surface, where the tip indents the material. A schematic representation of the used models can be seen in Figure 2.

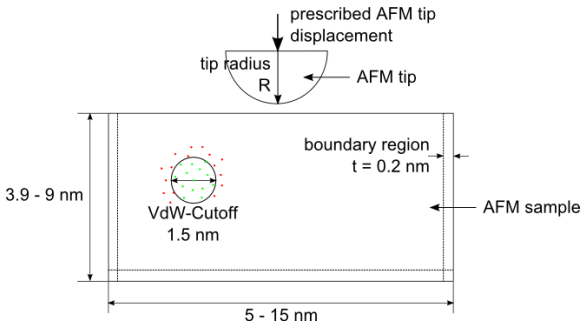

Figure 2: Schematic representation of the AFM models.

Due to the comparatively high numerical effort of MD simulations as well as MDFEM simulations, it is necessary to reduce the model size. The calculations for determining the interphase properties are performed on a 5 nm particle, which is considerably smaller than the primary particle size of approximately 14 nm observed in experiments. Minimum tip and sample sizes are obtained in preliminary simulations shown in the following section. To extract the interphase stiffnesses, the tip is shifted to the desired position in the global model after the relaxation step and subsequently the global model is reduced to a smaller submodel for each AFM-indent, as illustrated in Figure 3 a). After each shifting and reducing step, the 2 node elements representing the physical interactions are renewed and a short relaxation is performed. Then the actual load step is performed.

4 RESULTS AND DISCUSSION

As a result of the simulations, force-deformation curves are obtained. The Young's Modulus is then calculated through a Hertz fit similar to AFM experiments:

$$D = \left(\frac{F}{\sqrt{R} \cdot E_{tot}} \right)^{2/3} \tag{1}$$

with

$$\frac{1}{E_{tot}} = \frac{3}{4} \left(\frac{1 - {\nu_{tip}}^2}{E_{tip}} + \frac{1 - \nu^2}{E} \right), \tag{2}$$

where D is the deformation, F is the force acting on the cantilever beam (corresponding to $D_c \cdot k_c$ in the experiment, with the cantilever deflection D_c and the stiffness k_c of the cantilever beam), R is the tip radius and E_{tot} is the reduced elastic modulus of the series connection of tip and sample. If a rigid AFM tip is assumed, E_{tip} becomes infinite and the first term in the parenthesis in equation (2) vanishes. Combining Equation (1) and the reduced form of Equation (2) leads to

$$D = \left(\frac{3}{4} \cdot \frac{F(1 - \nu^2)}{\sqrt{R} E} \right)^{\frac{2}{3}}. \tag{3}$$

With E being the unknown parameter, Equation (3) is then fitted to the simulated curve applying a least square fit with MATLAB, as can be seen exemplarily in Figure 3 b).

The red dashed line in Figure 3 b) indicates the onset of a deviation between the fitted and simulated curve. This effect is caused by boundary effects (at a certain penetration the rigid boundaries start influencing the curve), indicating that the sample size in this example is chosen too small. To bypass this, either the sample size has to be increased or the range in which the Hertz fit is calculated has to be truncated (in this example the latter was already performed).

4.1 Preliminary Investigations

In preliminary investigations, AFM simulations on pure boehmite crystals and epoxy resin are performed in order to reexamine the assumptions like e.g. the crystal structure or the chosen force field. Additionally, the goal is to find the minimum model sizes (tip size, sample size), since model sizes have to be reduced due to the numerical limitations. Furthermore, the effect of the boundary conditions on the calculated elastic modulus is analyzed.

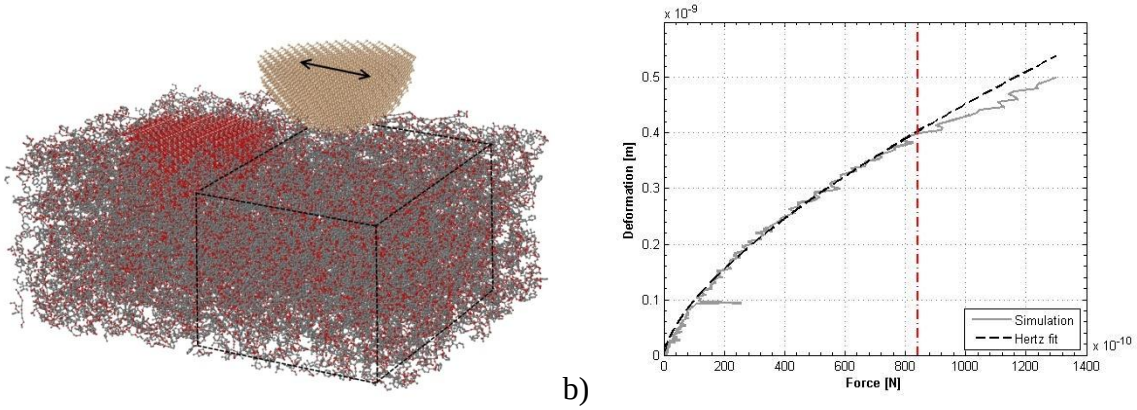

Figure 3: a) Example model of an AFM simulation (3 nm tip radius, 17.5 x 7.2 x 12 nm sample, approx. 90000 atoms, the black box indicates the minimum sample size, that is cut out prior to the loading step); b) Least square Hertz fit to simulated curve for the pure boehmite sample (red dashed line indicates onset of deviation between fitted and simulated curve caused by boundary effects).

To determine the minimum tip size, simulations with increasing tip radius (1 – 5 nm in steps of 1 nm) are performed for both materials. The boehmite is modeled with a sample size four times as big as the tip radius and the epoxy with a sample size of 15 x 9 x 15 nm. Both sample sizes are assumed to be large enough, not to impose any boundary effects on the measured modulus, which is shown to be valid in the following. The results concerning the effect of the tip radius on the calculated elastic modulus are depicted in Figure 4 a) for pure boehmite and Figure 4 b) for pure epoxy respectively.

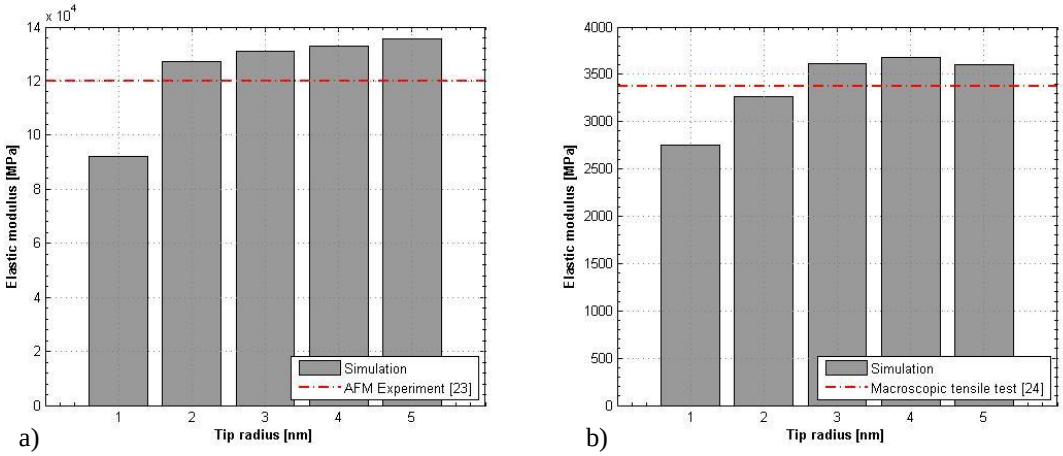

Figure 4: a) Influence of the AFM tip size on the calculated elastic modulus of pure boehmite crystals; b) Influence of the AFM tip size on the calculated elastic modulus of pure epoxy resin.

It is apparent, that with increasing tip radius the calculated moduli converge for both materials. Small tips underestimate the moduli, but already for 2 nm in case of the boehmite and for 3 nm in case of the epoxy the deviations between smaller and bigger tip sizes are smaller than 4 %. It can also be seen that the presented values are slightly above the displayed reference values from experimental investigations (13 % for the pure boehmite and 7 % for the pure epoxy). However, comparatively little literature on AFM tests on boehmite or the elastic properties of boehmite is available, making the comparison rather less reliable. The results for the pure epoxy are compared with results from macroscopic tensile tests.

The minimum sample size is determined using a similar approach. Starting with the full model size of 8 x 4.8 x 8 nm for boehmite and 15 x 9 x 15 nm for the epoxy resin, the sample size is gradually reduced to a minimum of 5 x 3 x 5 nm (boehmite) and 9 x 5.4 x 9 nm (epoxy). The aspect ratio remains the same for all samples. The simulations are performed with a 2 nm tip for the boehmite and a 3 nm tip for the epoxy. Figure 5 a) displays the resulting force-deformation curves for boehmite. As expected, with decreasing sample size, the point where the simulated curves start deviating from the Hertz curve is shifted to a lower deformation (marked by the straight lines in Figure 5 a)). Interestingly, reducing the model size from 8 to 6.5 nm and from 6.5 to 5 nm leads to an almost equal deformation shift of about 0.15 nm. The dashed simulation curve line in Figure 5 a) (denoted with Simulation "5x3 nm rcb", rcb = remove constrained bonds) represents a model, where some of the elements in the boundary region are deleted, as it is often done in MD simulations to soften the boundary conditions. All bond stretch elements and all angle bend and torsion elements with at least two nodes lying in the boundary region are deleted. With this model the deviation point can be shifted by approximately 0.09 nm, showing a good opportunity for model size reduction.

The results for pure epoxy in Figure 5 b) show significantly greater fluctuations, particularly the small models, which makes fitting the Hertz curve more difficult, especially for very small deformations. Thus, the deviation point is not as obvious as it is for boehmite. Therefore, simulations with greater tip displacements of 1.5 nm have been performed. The straight lines again represent the mark the onset of deviation from the Hertz curve. The line for the 9x5.4 nm variation is not displayed because it behaves too stiff from the beginning, whereas variation 15x9 nm shows good agreement in the whole range examined. A sample size of 12 x 7.2 x 12 nm is chosen to be the reference size for further investigations as a compromise between accuracy and efficiency. The "rcb" version has due to the fluctuations not been regarded during the following.

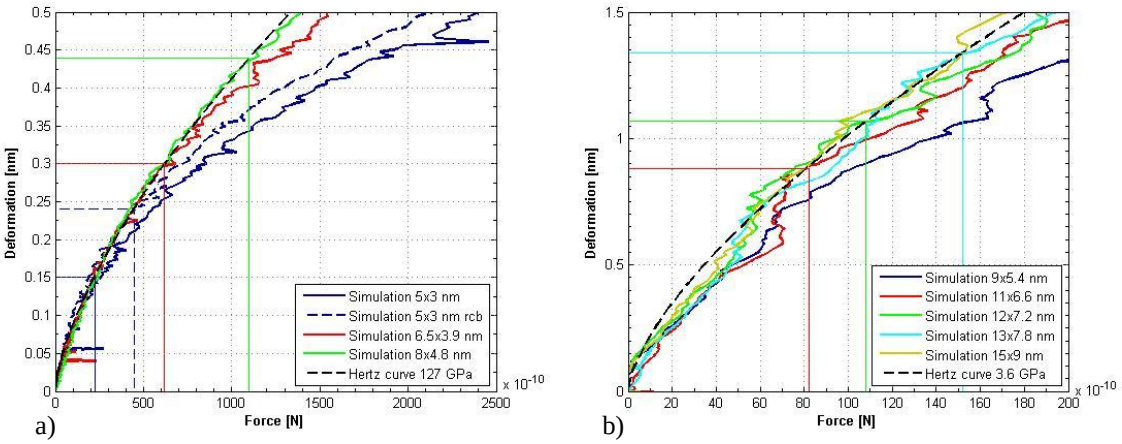

Figure 5: a) Influence of the sample size on the calculated elastic modulus of the pure boehmite crystal; b) Influence of the sample size on the calculated elastic modulus of the pure epoxy.

4.2 Nanocomposite AFM Simulation Results

Based on the findings of the previous chapter, in the following, the simulation results are shown for the combined particle-matrix samples. The tip size for the following models is chosen to be 3 nm and the sample size is 12 x 7.2 x 12 nm. The corresponding results are displayed in Figure 6. For each of the curves presented, 15 virtual AFM experiments are performed in a line in radial direction between 0 and 40 Å originating on the particle surface as illustrated in Figure 6 a). The region close to the particle surface can, as in real AFM exper-

iments, not be characterized, since depending on the tip size, tip flank and particle overlap. Thus a mix of particle and interphase modulus is measured in this case. Therefore, the particle surface appears to be shifted outward. Hence, in Figure 6 b) the region of 15 Å around the particle is neglected. Comparing the obtained curves of the interphase stiffnesses, the differences are clearly visible. The reference configuration, where the particle is not chemically but only physically bonded to the matrix, exhibits a constant stiffness and thus no visible interphase in the examinable region. This leads to the conclusion, that the particle does not influence the cross-linking in the surrounding matrix. Figure 6 c) shows the aforementioned behavior more demonstratively. It displays a stiffness plot, for which not the complete surface is screened, as in real AFM experiments, but the curve depicted in Figure 6 b) is rotated around the center of the particle. The coloring indicates the stiffness, with brighter regions being stiffer as darker regions. The red dashed circle displays the real particle surface. For the reference configuration, no interphase is visible. Variation 2 (hydroxyl groups on the particle surface are enabled to react during curing reaction, see Figure 6 d)) in contrast shows a clearly visible interphase. The region between 18 and 38 Å originating on the particle surface exhibits reduced stiffnesses by an amount of approximately 1 GPa (corresponding to a reduction of about 30 %). Further away from the particle surface the stiffness reaches the magnitude of the undisturbed matrix material. Variation 3 (with the pre-etherification step, see Figure 6 e)) exhibits an even more distinct interphase. The average reduction of the matrix stiffness is about 1.5 to 2 GPa (approximately 50 %). At the border of the used models the interphase stiffness is still reduced and thus the size of the interphase could not be determined.

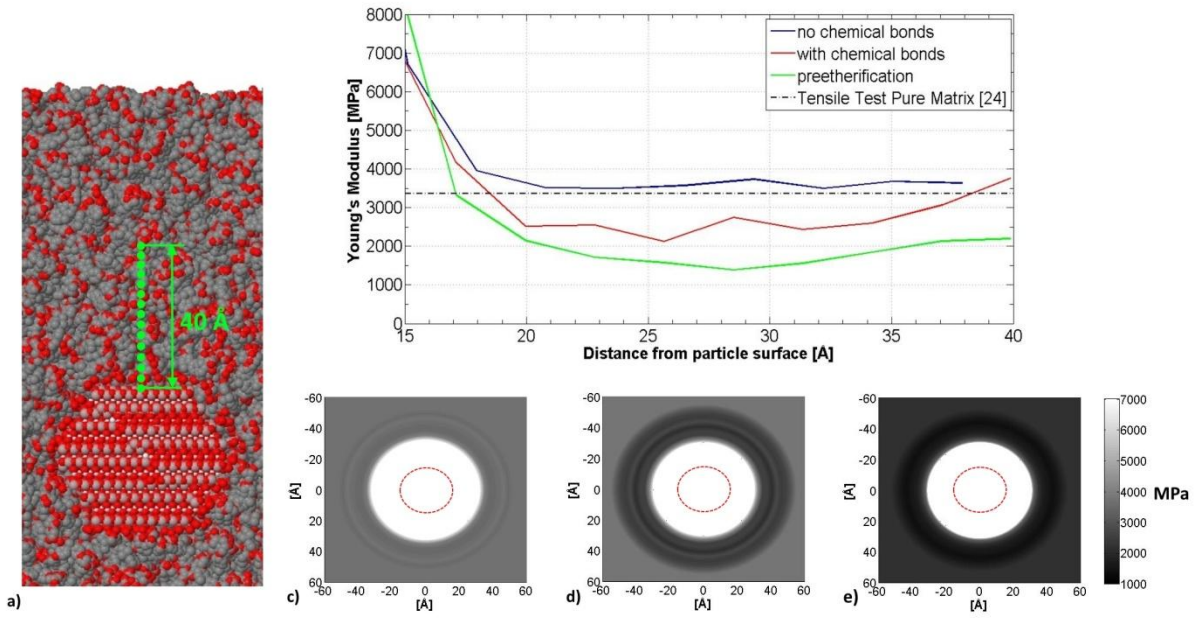

Figure 6: a) AFM measuring points; b) distribution of the interphase stiffness in dependency of the particle distance; c) stiffness plot without chemical interactions; d) stiffness plot with chemical interactions; e) stiffness plot with pre-etherification step (the red dashed circle indicates the real particle surface).

These results and their origins become more distinct in the context of the curing statistics of the underlying models (see Table 1). All models contain the same amount of epoxy groups and the same amount of hardener molecules is available for the cross-linking reaction. This results from the same particle geometry and weight fraction, leading to an equal amount of packed prepolymer chains. The values presented in Table 1 generally differ only by small

amounts, because the statistics refer to the complete model, not just to the interphase. However, the change of the values results mainly from the changed morphology of the interphase. All models have an almost equal amount of etherified connections. Interestingly the remaining curing statistics of the models of variation 2 and 3 show an opposite trend compared to the reference variation. This indicates different underlying mechanisms. For variation 2 (with chemical bonds but without a pre-etherification step), more hardener molecules are placed, leading to fewer monoesters. This is caused by the bigger amount of available hydroxyl groups, since particle surface hydroxyls are available additionally to the epoxy hydroxyls. Therefore in total more cross-links are created, but some cross-links are created between particle and matrix instead of within the matrix. This leads to a reduction of the matrix stiffness in the vicinity of the particle. In case of the pre-etherification step, the amount of hardeners used in the esterification step is significantly reduced. At the same time the number of monoesters and the number of epoxy molecules used show the highest value of the three variations. This is caused by the effect that many hydroxyl and epoxy groups are already occupied and no longer available for reaction. This leads to the conclusion, that in this case the cross-linking is really impeded, not just shifted to other reaction sites.

variation	Agent molecules used in esterification step [%]	Number of etherified connections	Number of Monoesters	Number of epoxy molecules used [%]
1: No chemical bonds	93.81	197	705	97.45
2: With chemical bonds	93.98	196	686	97.52
3: pre-etherification	93.45	196	746	97.67

Table 1: Curing statistics of the three compared variations.

4.3 Validation of Nanocomposite Materials

Since up to now the experimental results for a one-to-one comparison to the simulated AFM curves are not available yet, a statement about the variation that most likely fits the reality is made on the basis of simulated tensile tests. Therefore, cubic unit cells with 10 wt-% boehmite particles of 3 nm particle size are created and calculated (see Figure 7 a)). For each variation, three simulations with displacement boundary conditions in the three spatial directions have been performed and averaged. The results are shown and compared to the experimental result in Figure 7. It is obvious, that variation 2 matches the experimental result best. Variation 1 and 3 however, show good agreement among each other, but yield in a softer behavior than variation 2 and the experimental curve. The Young's modulus is extracted by fitting a straight line to the simulated curves in the strain range of 0.0002 to 0.01, leading to values of 3644 MPa, 3786 MPa and 3652 MPa for the variations 1, 2 and 3. The resulting Young's modulus of the experiment is calculated in the usual way between 0.0005 and 0.0025 with a value of 3806 MPa. Variation 2 shows an excellent agreement with the experimentally measured results.

The remaining question, why variation 3 does not show an even stiffer behavior than variation 3, but behaves almost similar to variation 1 can be answered as follows. In case of no chemical interactions, the particle is bonded to the matrix in a very weak way. This prevents an appropriate load transfer from the matrix into the particle. As can be seen from the curves in Figure 6 as well as from the curing statistics, variation 3 produces a very soft interphase. This leads to the conclusion, that in this variation in fact the particle-matrix interactions are

quiet strong, but at the cost of a very weak interphase, that, analogously to the weak bonding in case of variation 1, causes an unfavorable load transfer and thus a softer elastic behavior.

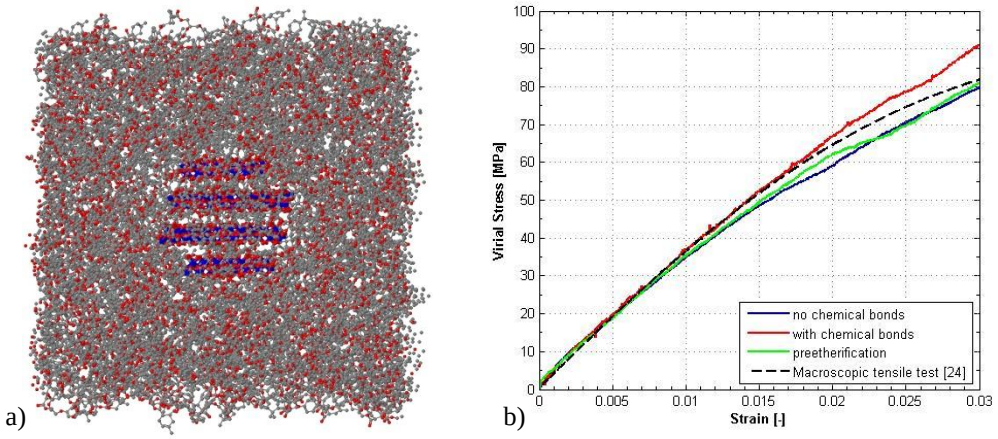

Figure 7: a) Example model for simulation of tensile test (3 nm particle, 8 nm boxsize, approx. 26000 atoms); b) Averaged stress-strain curves of a simulated tensile tests of an epoxy with 10 wt-% unmodified boehmite particles with 3 nm particle size in comparison with the experimentally obtained stress-strain curve.

5 CONCLUSION

The pure boehmite crystal and the pure epoxy have been investigated by atomic force microscopy simulations. The elastic moduli have been determined with 135 GPa for the boehmite and 3.6 GPa for the epoxy respectively. Both results show a good agreement with experimentally obtained values.

Furthermore, the influence of different particle-matrix interactions on the development of the mechanical properties in the particle matrix interphase has been studied. Three different variations were examined. Firstly, the particle was bonded by physical interactions only, secondly the surface hydroxyl groups of the boehmite particle were able to develop dative bonds during the curing reaction of the matrix. As a third variation, the surface hydroxyl groups were allowed to react with the epoxy groups of the matrix through etherification prior to the actual curing reaction. The first variation shows no visible interphase, leading to the conclusion that in this case the particle does not influence the cross-linking in the surrounding matrix. For the second variation, an interphase with a radius of approximately 38 Å and a mean stiffness reduction of approximately 30 % compared to the undisturbed matrix was obtained. Variation three shows an even more distinct interphase with a stiffness reduction of about 50% and an even bigger interphase size.

Since up to now no experimental data for the comparison to the simulated curves is available, numerical tensile test have been performed. The simulated tensile test of the variation containing chemical interactions between particle and matrix but no pre-etherification step yields in a quiet accurate prediction of the elastic behavior, whereas the variation with the pre-etherification step does not. Therefore in general the goal should be to find a balance between a good particle matrix interaction and the weakening of the interphase. Otherwise the problem of a poor load transfer is simply shifted away from the particle surface into the matrix.

The presented method can provide insight in the underlying mechanisms of nanoparticle reinforcements and significantly contribute to the optimization of nanocomposite materials, e.g. by investigating the influence of different particle surface modifications on the interphase properties. At the same time, in long term perspective, the technique is able to adequately replace AFM experiments and thus reduce the need of experimental effort. The goal of ongoing

studies is the investigation of varying surface modifications with varying parameters, like e.g. surface loading. Through parallel simulations of tensile tests, the influence of the composition and the developed mechanical properties within the interphase on the mechanical properties of the whole composite can be studied systematically. Furthermore, a direct comparison with real AFM experiments is pursued.

6 ACKNOWLEGEMENTS

This work originates from the Research Unit FOR 2021 "Acting Principles of Nano-Scaled Matrix Additives for Composite Structures". The authors would like to thank Benedikt Finke, Dr. Carsten Schilde and Professor Arno Kwade of the Institute for Particle Technology at the TU Braunschweig for providing and analyzing X-ray diffraction data of boehmite nanoparticles and Maximilian Jux and Professor Michael Sinapius of the Institute of Adaptronics and Function Integration at DLR Braunschweig for providing the experimental data of tensile tests of the pure/reinforced epoxy resin.

The Research Unit FOR 2021 is funded by the German Research Foundation (DFG). Furthermore the authors acknowledge the support by the RRZN scientific computing cluster, which is funded by the Leibniz Universität Hannover, the Lower Saxony Ministry of Science and Culture (MWK) and the German Research Foundation (DFG). The authors wish to express their gratitude for the financial support.

The pictures of the chemical unit cells and models in Figure 1, Figure 3 and Figure 7 are generated using Jmol [25], an open-source Java viewer for chemical structures in 3D.

REFERENES

[1] C. Arlt, Wirkungsweisen nanoskaliger Böhmite in einem Polymer und seinem Kohlenstofffaserverbund unter Druckbelastung. *Dissertation*, 2011.

[2] M.F. Uddin, C.T. Sun, Strength of unidirectional glass/epoxy composite with silica nanoparticle-enhanced matrix, *Composites Science and Technology*, 68(7-8), 1637-1643, 2008.

[3] A.K. Subramaniyan, C.T. Sun, Enhancing compressive strength of unidirectional polymeric composites using nanoclay, *Composites Part A: Applied Science and Manufacturing*, 37(12), 2257-2268, 2006.

[4] N. Shahid, R.G. Villate, A.R. Barron, Chemically functionalized alumina nanoparticle effect on carbon fiber/epoxy composites, *Composites Science and Technology*, 65(14), 2250-2258, 2005.

[5] N.A. Siddiqui, R.S.C. Woo, J.K. Kim, C.C.K. Leung, A. Munir, Mode I interlaminar behavior and mechanical properties of CFRPs with nanoclay-filled epoxy matrix, *Composites Part A: Applied Science and Manufacturing*, 38(2), 449-460, 2007.

[6] U. Landman, W.D. Luedke, N.A. Burnham, R.J. Colton, Atomistic Mechanisms and Dynamics of adhesion, Nanoindentation, and Fracture, *Sience*. 248, 454-461, 1990.

[7] T.-H. Fang, C.-I. Wenig, J.-G. Chang, Molecular dynamics simulation of nanolithography process using atomic force microscopy, *Surface Science*, 501(1-2), 138–147, 2002.

[8] B. Heymann, H. Grubmüller, AN02/DNP-hapten unbinding forces studied by molecular dynamics atomic force microscopy simulations, Chemical Physics Letters, 303 (1-2), 1-9, 1999.

[9] L. Nasdala, A. Kempe, R. Rolfes, The Molecular Dynamic Finite Element Method (MDFEM), *Computers, Materials & Continua*, 19(1), 57-104, 2010.

[10] L. Nasdala, A. Kempe, R. Rolfes, Are finite elements appropriate for use in molecular dynamic simulations?. *Composites Science and Technology*, 72(9), 989-1000, 2012.

[11] Q. Wang, Effective in-plane stiffness and bending rigidity of armchair and zigzag carbon nanotubes. *Int J Solids Struct*, 41, 5451-5461, 2004.

[12] H.W. Zhang, Z. Yao, J.B. Wang, W.X. Zhong. Phonon dispersion analysis of carbon nanotubes based on inter-belt model and symplectic solution method. *Int J Solids Struct*, 44, 6428-6449, 2007.

[13] S.Q. Zhu, X. Wang, Effect of Environmental Temperatures on Elastic Properties of Single-Walled Carbon Nanotube. *J Therm Stress*, 30, 1195-1210, 2007.

[14] C.Y. Li, T.W. Chou, A structural mechanics approach for the analysis of carbon nanotubes. *Int J Solids Struct*, 40, 2487-2499, 2003.

[15] M. Chwal, Influence of vacancy defects on the mechanical behavior and properties of carbon nanotubes, *Proc Eng*, 10, 1579-1584, 2011.

[16] E.I. Saavedra Flores, S. Adhikari, M.I. Friswell, F. Scarpa, Hyperelastic finite element model for single wall carbon nanotubes in tension. *Comput Mater Sci*, 50(3), 1083-1087, 2011.

[17] L. Nasdala, A. Kempe, R. Rolfes, An elastic molecular model for rubber inelasticity. *Comput Mater Sci*, 106, 83-99, 2015

[18] X. Bokhimi, J.A. Toledo-Antonio, M.L. Guzmán-Castillo, F. Hernández-Beltrán, Relationship between Crystallite Size and Bond Length in Boehmite. *J Solid State Chem*, 159(1), 32-40, 2001.

[19] B. Finke, Institute for Particle Technology, TU Braunschweig (private communication)

[20] N.M. O'Boyle, M. Banck, C.A. James, C. Morley, T. Vandermeersch, and G.R. Hutchison. Open Babel: An open chemical toolbox. *J. Cheminf*, 3-33,2011

[21] L. Martínez, R. Andrade, E. G. Birgin, J. M. Martínez. Packmol: A package for building initial configurations for molecular dynamics simulations. *J Comp Chem*, 30(13), 2157-2164, 2009.

[22] S.L. Mayo, B.D. Olafson, W.A. Goddard, DREIDING: a generic force field for molecular simulations. *J Phys Chem*, 94(26), 8897-8909, 1990.

[23] R.C. Streller, Boehmite als Nanofüllstoffe für Polypropylen-Nanocomposites und Nanopartikel-modifizierte Polypropylen/Kautschuk-Blends. *Dissertation*, 2008.

[24] M. Jux, Institute of Adaptronics and Function Integration, DLR Braunschweig (private communication)

[25] Jmol: an open-source Java viewer for chemical structures in 3D. http://www.jmol.org/